Gait & Posture 64 (2018) 205–212

Contents lists available at ScienceDirect

Gait & Posture

journal homepage: www.elsevier.com/locate/gaitpost

Full Length Article

Quantification of multi-segment trunk kinetics during multi-directional trunk bending

Alireza Noamani[a], Albert H. Vette[a,b], Richard Preuss[c], Milos R. Popovic[d], Hossein Rouhani[a,*]

[a] Department of Mechanical Engineering, University of Alberta, Donadeo Innovation Centre for Engineering, Edmonton, Alberta, T6G 1H9, Canada
[b] Glenrose Rehabilitation Hospital, Alberta Health Services, 10230 111 Avenue NW, Edmonton, Alberta, T5G 0B7, Canada
[c] School of Physical & Occupational Therapy, McGill University, Montreal, Quebec, H3G 1Y5, Canada
[d] Rehabilitation Engineering Laboratory, Lyndhurst Centre, Toronto Rehabilitation Institute –University Health Network, Toronto, Ontario, M4G 3V9, Canada

ARTICLE INFO

Keywords:
Inverse dynamics
Joint moments
Multi-segment model
Trunk kinetics

ABSTRACT

Background: Motion assessment of the body's head-arms-trunk (HAT) using linked-segment models, along with an inverse dynamics approach, can enable in vivo estimations of inter-vertebral moments. However, this mathematical approach is prone to experimental errors because of inaccuracies in (i) kinematic measurements associated with soft tissue artifacts and (ii) estimating individual-specific body segment parameters (BSPs). The inaccuracy of the BSPs is particularly challenging for the multi-segment HAT due to high inter-participant variability in the HAT's BSPs and no study currently exists that can provide a less erroneous estimation of the joint moments along the spinal column.
Research question: This study characterized three-dimensional (3D) inter-segmental moments in a multi-segment HAT model during multi-directional trunk-bending, after minimizing the experimental errors.
Method: Eleven healthy individuals participated in a multi-directional trunk-bending experiment in five directions with three speeds. A seven-segment HAT model was reconstructed for each participant, and its motion was recorded. After compensating for experimental errors due to soft tissue artifacts, and using optimized individual-specific BSPs, and center of pressure offsets, the inter-segmental moments were calculated via inverse dynamics.
Results: Our results show a significant effect of the inter-segmental level and trunk-bending directions on the obtained moments. Compensating for soft tissue artifacts contributed significantly to reducing errors. Our results indicate complex, task-specific patterns of the 3D moments, with high inter-participant variability at different inter-segmental levels, which cannot be studied using single-segment models or without error compensation.
Significance: Interpretation of inter-segmental moments after compensation of experimental errors is important for clinical evaluations and developing injury prevention and rehabilitation strategies.

1. Introduction

Accurate estimation of the intra-spinal loads is essential for assessing the risk of injury during occupational and daily activities, as well as for designing prevention and treatment strategies [1], and pre- and post-treatment assessments [2]. The three-dimensional (3D) kinematics of the upper body have been widely investigated using one-segment and multi-segment models of the head-arms-trunk (HAT) [3]. However, direct *in vivo* measurement of the inter-vertebral forces and moments requires minute transducers inserted around the spine, which is not feasible for real-world, clinical measurements. Therefore, researchers use indirect estimation of kinetic variables via mathematical techniques, such as inverse dynamics, along with linked-segment models.

Several studies have used an indirect estimation approach to compute the 3D reaction forces and moments at the lumbo-sacral ($L5/S1$) joint with a one-segment HAT model during walking [4,5], lifting [6], balance recovery [7], and sit-to-stand [8], as well as for clinical evaluation of low-back pain [4,6] and lower-limb amputation [5]. Regression equations [4,9,10], scaling equations [7], or geometrical models [1] have been used for estimating body segment parameters (BSPs) of a one-segment HAT model. These studies investigated lumbo-sacral moments using a single-segment HAT model. On the other hand, multi-segment HAT kinetics have rarely been investigated. Recently, Seay et al. [11] used a two-segment HAT model to estimate the joint moments acting at $L5/S1$ and $T12/L1$ during running. They assumed a cylindrical thorax segment and calculated the lumbar segment's BSPs

* Corresponding author at: Department of Mechanical Engineering, University of Alberta, 10-368 Donadeo Innovation Centre for Engineering, 9211-116 Street NW, Edmonton, AB T6G 1H9, Canada.
E-mail address: hrouhani@ualberta.ca (H. Rouhani).

https://doi.org/10.1016/j.gaitpost.2018.06.027
Received 15 December 2017; Received in revised form 8 June 2018; Accepted 11 June 2018

according to Pearsall et al. [12]. A more recent study [13] investigated the test-retest reliability of 3D two-segment HAT (lumbar and thoracic) kinematics and kinetics during gait. They used a biomechanical model of the body according to Seay et al. [11] and determined the BSPs of the trunk segments based on Pearsall et al. [12].

The main challenge in extending one- and two-segment models to the assessment of multi-segment HAT kinetics relates to the complexities in estimating individual-specific BSPs and the 3D motion of several small segments along the spinal column. Preuss et al. [14] compared seven-segment HAT kinematics to those of one- and two-segment models and concluded that a seven-segment model captures complex motion patterns that are omitted by one- and two-segment models. As such, we expect that a multi-segment model can capture kinetic patterns that cannot be captured by one- and two-segment models. Multi-segment HAT kinetics require measurements of the inter-segmental motions and ground reaction forces (GRF), as well as accurate BSPs estimation. Although inverse dynamics are commonly used to assess human body kinetics, this procedure is error-prone. These errors are because of inaccuracies in (a) motion data [15], (b) force plate measurements [16], and (c) BSPs estimation [17], which can cause errors ranging up to 232% in the estimated peak moment [18]. A sensitivity to errors of the computed lumbo-sacral joint moment [19], especially due to BSPs inaccuracy [7], was observed when a one-segment HAT model was used. Strategies to compensate for these inaccuracies could enable a more reliable estimation of the inter-vertebral moments. However, due to technical challenges, these strategies are not trivial, particularly for assessing multi-segment HAT kinetics. Two of these challenges are discussed below.

First, the relative motion between skin-mounted markers and bony prominences, i.e., soft tissue artifacts (STAs), during dynamic tasks causes inaccuracy in obtained joint angles [2,20]. Hence, the assessment of the inter-vertebral moments via an inverse dynamics approach is likely affected by STAs. Previous studies have shown the considerable impact of STAs on the measurement accuracy of lower limb kinematics and kinetics [21,22], and kinematics of the scapula [23] and spine [2]. However, to our knowledge, no study has quantified the STA effect on the inter-segmental joint moments of a multi-segment HAT model. Compensating the STA effect could reduce the error in the HAT kinematics assessment and result in a less erroneous joint moment estimation using inverse dynamics.

Second, assessing HAT kinetics via inverse dynamics requires an accurate estimation of individual-specific BSPs, including the 3D center of mass (COM) coordinates, 3D coordinates of the joint's center of rotation (JCR), and the mass and moments of inertia for each segment. Estimations of individual-specific BSPs using predictive equations based on medical imaging [24] and cadaveric data [25] were proposed. However, these estimations may induce errors of over 40% in the joint moment estimation [17]. To minimize the effect of the BSPs' inaccuracy, optimization methods have been proposed in calculating net joint moments at lower limb joints in the sagittal plane [17]. However, to our knowledge, no study has estimated the 3D joint moments of a multi-segment HAT model based on optimized individual-specific BSPs. A less erroneous estimation of individual-specific BSPs could enable a more reliable estimation of the inter-vertebral moments. Our team has recently obtained detailed BSPs for each vertebra from a single cadaver to calculate the moments at spinal joints using a multi-segment HAT model [26]. However, the obtained kinetic results might be considerably affected by the heterogeneity of BSPs between individuals. Later, we presented a novel method [27] to obtain optimized individual-specific BSPs of the HAT segments and proposed it as a less erroneous estimation of the 3D inter-segmental moments of the spinal column.

Building upon these efforts, the present study has two main aims: (1) to quantify multi-segment trunk kinetics after experimental error minimization, based on optimized, participant-specific BSPs and STA error compensation; (2) characterize the effect of STAs on the inter-segmental moments across different spinal joints and trunk-bending directions using two commonly-used inverse dynamics approaches (bottom-up and top-down); and (3) quantify moment variations across the spine during different trunk-bending directions. Previous studies have assessed the joint moment at the lumbo-sacral joint during walking [5], lifting [9], lowering objects [6], and sit-to-stand [8]. However, to quantify moment variations at different levels of the spinal column, distinguishable moments at different joint levels were required. Trunk-bending in different directions not only results in large, distinguishable moments at different joint levels, but also helps us to study the contribution of different moment components (sagittal, coronal, and transverse) toward the net joint moment.

2. Methods

2.1. Experimental procedures

The experimental procedures were described in detail in our previous study [14] and are only briefly described here. Eleven healthy individuals (4 females and 7 males; age: 28.5 ± 3.3 years; trunk height: 0.75 ± 0.04 m; body mass: 69.9 ± 13.7 kg) with no history of persistent back pain or spine-related musculoskeletal or neuromuscular impairments participated in the experiment. All participants provided written consent prior to participating in the study. Research Ethics Board approval was received from the university research ethics committee.

Participants sat naturally on a rigid, elevated force-plate, with their lower legs freely hanging with no constraints or support to restrict their movement. Five targets were placed anterior of the participant, with the distances and heights adjusted to elicit angular trunk motions of 45 °, based on the participant's trunk height (Fig. 1a). Participants were instructed to first look at the target, then lean toward the target, touch the target with their head, and then return to the initial upright sitting position. Although they initially rotated their head/trunk to look at the target, they did not perform compound flexion/rotation motion during the arc movement. Each participant randomly performed the tasks with three different speeds, paced by a metronome at 10, 20, and 30 degrees/s, for each target, three times for each speed. Through each trial, the arms were crossed, motionless over the chest.

Data acquisition and seven-segment HAT modeling (see Fig. 1b for joint definitions) were described in our previous study [14] and, thus, are only briefly described here.

2.2. Data acquisition

Twenty-one reflective markers were placed over and around the participant's spinal column to form a multi-segment HAT model (Fig. 1b). Six motion capture cameras (Vicon, Oxford, UK) recorded the position of the markers at a sampling frequency of 120 Hz A force plate (AMTI, Watertown, MA, USA) recorded the ground reaction forces (GRFs) and center of pressure (COP) position, at a sampling rate of 1000 Hz. The time-series of the marker trajectories and the force plate data were filtered using an 8th-order, dual-pass Butterworth low-pass filter (cut-off frequency: 2 Hz and 5 Hz, respectively).

2.3. Multi-segment model of the HAT

Seven rigid segments, defined using markers on the spine, were assumed to be connected to each other at the center of respective inter-vertebral discs (Fig. 1b). The proposed HAT model consisted of the head-neck (HD), upper thoracic (UT), mid-upper thoracic (MUT), mid-lower thoracic (MLT), lower thoracic (LT), upper-lumbar (UL), and lower lumbar (LL) segments. For each segment, the axes of a segment-fixed frame were defined using the locations of three markers: (1) the X-axis from left to right, parallel to the two markers placed laterally at 5 cm from the spinous process of the rostral vertebra, (2) the Z-axis

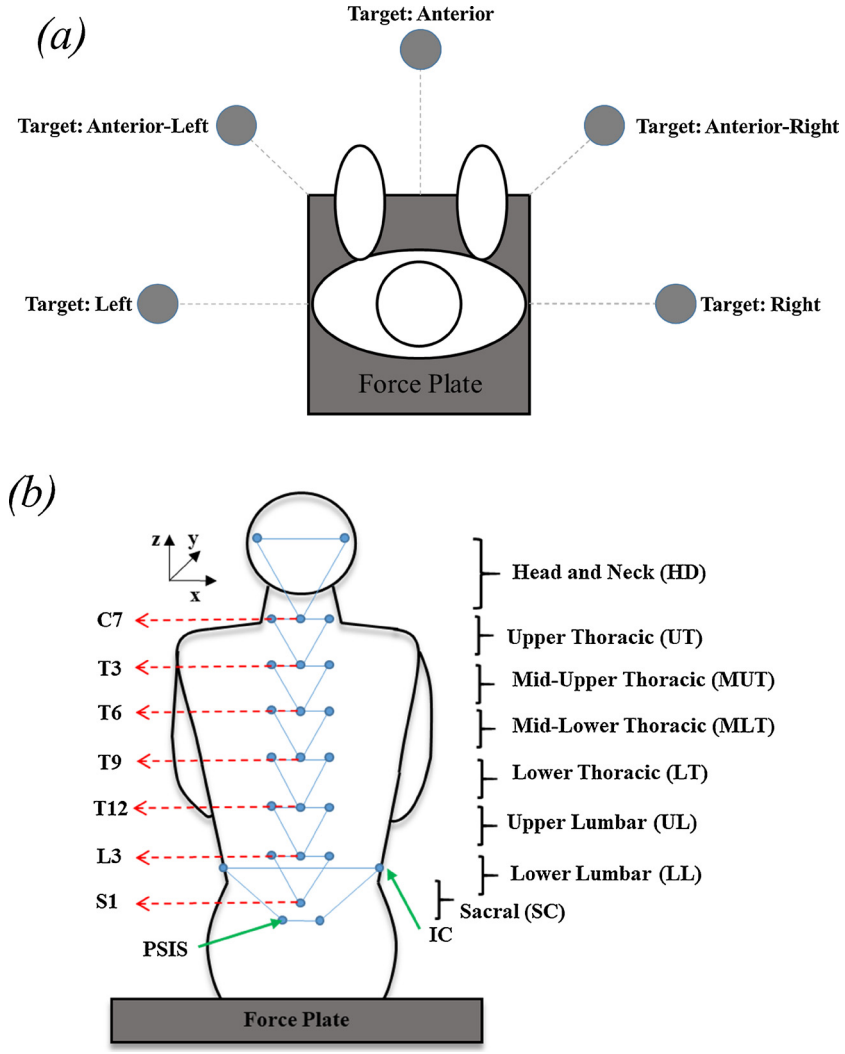

Fig. 1. (a) Targets for movement tasks. Targets were placed in the transverse plane at 45 ° intervals, anteriorly and laterally of the participant. To avoid a counterweight effect of the lower legs during trunk movement, participants kept their lower legs vertically downwards throughout the experiment. (b) Markers were placed over the spinal column to form a seven-segment trunk model: Head and neck (HD), upper thoracic (UT), mid-upper thoracic (MUT), mid-lower thoracic (MLT), lower thoracic (LT), upper lumbar (UL), lower lumbar (LL), and sacral (SC) segments.

pointing superiorly, parallel to the line between the marker placed on the spinous process of the caudal vertebra and the mid-point of two rostral markers, and (3) the Y-axis pointing anteriorly (Fig. 1b). Hence, the X-, Y-, and Z-axes represented flexion/extension, lateral bending, and axial rotation, respectively. The three markers that defined the pelvis-fixed frame were placed on the left and right iliac crests and the midpoint between the posterior superior iliac spines (PSIS). We compensated for errors in kinematics data induced by the STA for each individual, based on the technique described in Supplementary Material A and as described in our previous study [2].

2.4. Inverse dynamics

We implemented the Newton-Euler formulation for joint moment calculation in a custom-built code. Two approaches were used: (1) the bottom-approach that uses kinematics, BSPs, and GRFs to calculate the joint moments from the bottom-most joint and then proceeds upward, and (2) the top-down approach that uses kinematics and BSPs of the segments and calculates the joint moments from the top-most joint and then proceeds downward.

2.5. Optimized estimation of individual-specific BSPs for inverse dynamics

3D inter-segmental forces and moments were calculated through both bottom-up, and top-down inverse dynamics approaches. For this purpose, we used individual-specific scaling of the cadaveric data from the Male Visible Human images reported by Vette et al. [28], using body weight and trunk height of each participant to develop an initial guess of the BSPs of each HAT segment, i.e., mass, center of mass (COM), joint center of rotation (JCR), and moments of inertia. The trunk height of each participant was defined as the length of the line between the S1 and C7 markers. However, such scaling methods are error-prone when the data are applied to individuals with a different range of age, body type, sex and ethnicity [29,30]. Therefore, due to inaccurate estimations of BSPs for HAT segments, obtained using these scaling methods, the top-down and bottom-up inverse dynamics approaches were expected to result in different values for the net joint moments. Therefore, we adjusted the scaled BSPs to estimate an optimal individual-specific set of BSPs and the force plate COP offset by employing an optimization-based method. This optimization minimized the difference between the inter-segmental moments, which were obtained by top-down and bottom-up inverse dynamics approaches [27]. Our optimization method assumed constant mass, locations of the JCR and the segment COM (both locations relative to the segment-fixed

coordinate system) throughout the movement. Therefore, we assumed that the BSPs do not vary frame-by-frame.

2.6. Data analysis

The Kolmogorov-Smirnov test was used to determine whether the participants' calculated moments fell into normal distribution. Moreover, the Levene's test was used to assess the equality of variance in the case of normality. Statistical analysis of the inter-segmental moments in the sagittal, coronal, and transverse planes was conducted separately using a three-way analysis of variance (ANOVA). The independent variables were joint level (seven joints), target direction (five directions), and bending speed (three speeds), with the 3D joint moment being the dependent variable. In addition, to investigate the influence of STAs on the net joint moments, a two-way ANOVA was performed on the root-mean-square (RMS) difference between the net joint moment before and after STA error compensation. The independent variables were joint level and target direction, with the test being performed for both bottom-up and top-down inverse dynamic approaches.

All statistical analyses were performed on the absolute peak values of the 3D joint moments, with the significance level set at 0.01 when applying Bonferroni correction. A multiple comparison, post-hoc test was performed to investigate the main effects on the joint moments of the multi-segment HAT. Finally, the inter-participant variability of the peak moments was defined based on the coefficient of variation ($CV\% = \frac{standard\ deviation}{mean} \times 100$) amongst all participants.

3. Results

The CV% of the peak moments (indicator of inter-participant variability) varied from 27.3 to 82.1%, 7.5 to 72.2%, and 27.9 to 59.3% across different joints for the sagittal, coronal, and transverse moments, respectively (Table 1 and Fig. S1). We also observed the main effect of joint level and trunk-bending direction for moments in the sagittal, coronal, and transverse planes (Tables 1–3).

3.1. Effect of joint level

The sagittal moments of the lumbar joints (SC ~ LL, LL ~ UL, and UL ~ LT) were significantly larger ($p < 0.01$) compared to all other superior (thoracic and cervical) joints (Tables 1 and 2a). Among the lumbar joints, the sagittal moment at LL ~ UL tended to be the largest. Similarly, larger coronal moments were observed at inferior joints, relative to their superior joints, except for the coronal moment at SC ~ LL, which was larger than that of other joints, except the LL ~ UL joint. The transverse moment at the two most superior joints (MUT ~ UT and UT ~ HD) tended to be larger compared to the inferior joints, while no significant differences were found amongst the transverse moments at the inferior joints. The transverse moment in UT ~ HD was significantly larger compared to all inferior joints, except MUT ~ UT.

3.2. Effect of trunk-bending direction

Because it was larger in anterior direction than all other directions ($p < 0.01$), the sagittal moment across different joints decreased in more lateral trunk-bending directions compared to more anterior directions. No significant bilateral asymmetry was observed in the sagittal moments ($p = 1.00$) (Table 3a). The largest coronal moments were observed for trunk-bending in the lateral (left and right) directions. Again, no significant bilateral asymmetry was observed in the coronal moments (Table 3b).

3.3. Effect of the STA error compensation

There were significant main effects of joint level, and trunk-bending direction, as well as their interaction effect, on the RMS difference between the inter-segmental net joint moments, calculated before and after STA error compensation. This was observed for both bottom-up and top-down approaches (Tables 4 and 5). Results also reflected a significant difference between the influences of STA compensation on joint moments obtained via the two inverse dynamics approaches.

The main effect of speed on the sagittal, coronal, and transverse moments are presented in Supplementary Material B.

4. Discussion

Inverse dynamics approaches have been extensively used to estimate the lumbo-sacral joint moment, using a single-segment trunk model with regressions [4,9,10,19], scaling equations [7], or geometrical models [1] for estimating BSPs. However, multi-segment trunk kinetics have rarely been investigated. This is due to the technical challenges in minimizing the propagation of experimental errors: (i) inaccuracies in motion data (e.g., STA-induced error); and (ii) erroneous estimations of individual-specific BSPs for each trunk segment, due to the high inter-participant variability of the trunk's BSPs. No study has investigated the STA effects on the kinetics of the multi-segment HAT model. We have recently developed a methodology to compensate for the STA effects on the kinematics of the multi-segment HAT model, which can subsequently be used for joint moment

Table 1
Peak joint moments calculated via a bottom-up inverse dynamics approach using optimized individual-specific BSPs and STA-induced error compensation. The results are expressed as mean (coefficient of variations %) across all participants for inter-segmental joint moments at the sagittal, coronal, and transverse plane for five trunk-bending directions (see Fig. 1). The average of the three trials was used. Moments (N.m) were normalized by participant's body weight and trunk height. Moments were calculated with respect to the global frame of reference.

		SC ~ LT	LL ~ UL	UL ~ LT	LT ~ MLT	MLT ~ MUT	MUT ~ UT	UT ~ HD
Left	Sagittal	6.6 (31.7)	6.6 (33.7)	5.3 (38.0)	4.7 (48.4)	4.8 (47.9)	4.7 (44.3)	3.4 (81.5)
	Coronal	15.2 (10.8)	16.0 (8.9)	14.4 (9.2)	12.2 (9.5)	10.2 (12.0)	8.4 (15.9)	6.3 (30.0)
	Transverse	1.5 (28.6)	1.6 (27.9)	1.5 (30.2)	1.4 (31.3)	1.3 (32.9)	1.3 (33.9)	1.5 (30.9)
Anterior-Left	Sagittal	13.4 (40.0)	14.7 (34.4)	12.7 (40.5)	10.0 (39.6)	7.7 (39.5)	6.1 (37.6)	4.7 (60.9)
	Coronal	13.0 (13.3)	14.3 (14.5)	12.3 (16.0)	9.0 (19.5)	6.7 (26.6)	5.1 (33.9)	4.1 (48.7)
	Transverse	1.3 (41.5)	1.3 (42.2)	1.3 (43.4)	1.2 (45.2)	1.2 (46.5)	1.2 (47.8)	1.4 (45.1)
Anterior	Sagittal	17.3 (33.3)	18.9 (27.3)	15.3 (34.1)	10.7 (42.8)	7.6 (46.3)	5.9 (47.4)	4.6 (60.4)
	Coronal	1.8 (48.0)	1.8 (61.6)	1.5 (72.2)	1.5 (64.1)	1.4 (53.1)	1.4 (44.1)	1.3 (50.8)
	Transverse	0.9 (58.5)	0.9 (59.3)	0.9 (58.7)	1.0 (58.1)	1.2 (56.7)	1.3 (54.6)	1.5 (52.1)
Anterior-Right	Sagittal	13.5 (40.8)	15.0 (35.4)	12.8 (39.8)	9.6 (43.2)	7.2 (49.4)	5.7 (52.1)	4.5 (69.0)
	Coronal	13.5 (10.3)	14.9 (7.6)	12.7 (7.5)	8.8 (11.9)	6.1 (16.5)	4.1 (28.6)	3.1 (49.8)
	Transverse	1.8 (32.2)	1.8 (33.8)	1.9 (34.7)	2.0 (35.4)	2.1 (35.2)	2.3 (34.8)	2.6 (33.4)
Right	Sagittal	6.5 (29.7)	6.4 (30.9)	5.5 (44.1)	5.1 (53.9)	4.9 (59.5)	4.8 (57.6)	3.6 (82.1)
	Coronal	15.4 (13.6)	16.2 (13.6)	14.3 (12.1)	11.6 (15.5)	9.2 (20.1)	7.0 (28.5)	4.8 (52.9)
	Transverse	1.7 (35.3)	1.8 (35.4)	1.7 (37.6)	1.7 (38.5)	1.8 (39.5)	1.9 (39.0)	2.1 (34.8)

Table 2
The main effect of joint level on the sagittal moment (a), coronal moment (b), and transverse moment (c). * indicates significant differences ($p < 0.01$) in moments between individual pairs of joints.

(a) Effect of joint level on the sagittal moment

Joints	SC ~ LL	LL ~ UL	UL ~ LT	LT ~ MLT	MLT ~ MUT	MUT ~ UT	UT ~ HD
SC ~ LL				*	*	*	*
LL ~ UL			*	*	*	*	*
UL ~ LT		*		*	*	*	*
LT ~ MLT	*	*	*		*	*	*
MLT ~ MUT	*	*	*	*			*
MUT ~ UT	*	*	*	*			
UT ~ HD	*	*	*	*	*		

(b) Effect of joint level on the coronal moment

Joints	SC ~ LL	LL ~ UL	UL ~ LT	LT ~ MLT	MLT ~ MUT	MUT ~ UT	UT ~ HD
SC ~ LL		*	*	*	*	*	*
LL ~ UL	*		*	*	*	*	*
UL ~ LT	*	*		*	*	*	*
LT ~ MLT	*	*	*		*	*	*
MLT ~ MUT	*	*	*	*		*	*
MUT ~ UT	*	*	*	*	*		*
UT ~ HD	*	*	*	*	*	*	

(c) Effect of joint level on the transverse moment

Joints	SC ~ LL	LL ~ UL	UL ~ LT	LT ~ MLT	MLT ~ MUT	MUT ~ UT	UT ~ HD
SC ~ LL						*	*
LL ~ UL						*	*
UL ~ LT							*
LT ~ MLT							*
MLT ~ MUT							*
MUT ~ UT	*	*					
UT ~ HD	*	*	*	*	*		

calculation. Further, previous studies have shown the effects of inaccurate BSPs on the assessment of lower limb kinetics. We have recently proposed an optimization-based method for minimizing errors in joint moment calculation by estimating the individual-specific BSPs of a multi-segment HAT model. These two recently developed approaches enable us to assess, for the first time, the 3D kinetics of a multi-segment HAT model during multi-directional trunk-bending. Building on these previous studies, we obtained less erroneous estimations of the 3D

Table 3
The main effect of trunk-bending direction on the sagittal moment (a), coronal moment (b), and transverse moment (c). * indicates significant differences ($p < 0.01$) in moments between two directions.

(a) Effect of trunk-bending direction on the sagittal moment

Directions	Left	Anterior-Left	Anterior	Anterior-Right	Right
Left		*	*	*	
Anterior-Left	*		*		*
Anterior	*	*		*	*
Anterior-Right	*		*		*
Right		*	*	*	

(b) Effect of trunk-bending direction on the coronal moment

Directions	Left	Anterior-Left	Anterior	Anterior-Right	Right
Left		*	*	*	
Anterior-Left	*		*		*
Anterior	*	*		*	*
Anterior-Right	*		*		*
Right		*	*	*	

(c) Effect of trunk-bending direction on the transverse moment

Directions	Left	Anterior-Left	Anterior	Anterior-Right	Right
Left				*	*
Anterior-Left				*	*
Anterior				*	*
Anterior-Right	*	*	*		*
Right	*	*	*	*	

Table 4
RMS difference between the inter-segmental net joint moment calculated before and after STA error compensation at each joint level of the proposed HAT model for five trunk-bending directions (Fig. 1). Results are expressed as mean ± standard deviation among all participants and obtained through both (a) bottom-up and (b) top-down inverse dynamics approaches. The average of the three trials and three speeds are presented. Moments (N.m) were normalized by participant's body weight and trunk height. Moments were calculated with respect to the global frame of reference.

(a) Bottom-up approach

	SC ~ LT	LL ~ UL	UL ~ LT	LT ~ MLT	MLT ~ MUT	MUT ~ UT	UT ~ HD
Left	7.4 ± 1.4	7.5 ± 1.2	6.5 ± 0.9	5.5 ± 0.7	4.6 ± 0.9	3.9 ± 1	2.8 ± 1
Anterior-Left	8.2 ± 1.3	8.4 ± 0.9	7 ± 1.1	5.4 ± 0.9	3.7 ± 0.7	2.7 ± 0.8	2 ± 1
Anterior	8.4 ± 1.8	8.8 ± 1.3	6.8 ± 1.4	4.8 ± 1	2.8 ± 0.8	1.5 ± 0.7	1.4 ± 0.7
Anterior-Right	8.2 ± 1.5	8.5 ± 1.1	7 ± 1.1	5.3 ± 0.7	3.7 ± 0.6	2.8 ± 0.7	2.2 ± 0.8
Right	7.4 ± 1.1	7.5 ± 1	6.6 ± 0.7	5.6 ± 0.7	4.8 ± 1	4.1 ± 1.1	2.9 ± 1.3

(a) Top-down approach

	SC ~ LT	LL ~ UL	UL ~ LT	LT ~ MLT	MLT ~ MUT	MUT ~ UT	UT ~ HD
Left	5.4 ± 2	5.5 ± 1.8	4.5 ± 1.2	3.5 ± 0.9	2.6 ± 0.7	1.8 ± 0.8	0.6 ± 0.4
Anterior-Left	6.6 ± 2.1	6.9 ± 1.8	5.5 ± 1.6	4 ± 1.2	2.4 ± 0.7	1.4 ± 0.5	0.6 ± 0.4
Anterior	7.5 ± 2.5	7.9 ± 2.1	6 ± 1.8	4.2 ± 1.3	2.2 ± 0.8	1 ± 0.6	0.6 ± 0.3
Anterior-Right	6.8 ± 2.5	7.1 ± 2.1	5.6 ± 1.9	4 ± 1.2	2.4 ± 0.7	1.4 ± 0.5	0.6 ± 0.3
Right	5.4 ± 1.7	5.5 ± 1.5	4.5 ± 1.1	3.5 ± 0.8	2.6 ± 0.7	1.9 ± 0.7	0.6 ± 0.3

intervertebral moments based on optimized individual-specific BSPs, along with compensation of STA-induced errors. This method can facilitate the assessment of multi-segment trunk kinetics and enable objective clinical evaluations and decision-making. Notably, previous studies have investigated the joint moment at the $L5/S1$ joint. Hendershot and Wolf [8] reported a peak normalized sagittal moment of 1.78 ± 0.28 N·m/kg at the $L5/S1$ joint among healthy individuals during sit-to-stand. Plamondon et al. [9] reported a peak sagittal

Table 5
The main effect of joint level and trunk-bending direction on the RMS difference between the inter-segmental net joint moment before and after STA error compensation calculated via bottom-up, and top-down approaches. * indicates significant differences ($p < 0.01$) in the moments between individual pairs of joints.

(a) Effect of joint level on the RMS difference calculated via bottom-up approach

Joints	SC ~ LL	LL ~ UL	SC ~ LL	LL ~ UL	MLT ~ MUT	MUT ~ UT	UT ~ HD
SC ~ LL			*	*	*	*	*
LL ~ UL			*	*	*	*	*
UL ~ LT	*	*		*	*	*	*
LT ~ MLT	*	*	*		*	*	*
MLT ~ MUT	*	*	*	*		*	*
MUT ~ UT	*	*	*	*	*		*
UT ~ HD	*	*	*	*	*	*	

(b) Effect of joint level on the RMS difference calculated via top-down approach

Joints	SC ~ LL	LL ~ UL	SC ~ LL	LL ~ UL	MLT ~ MUT	MUT ~ UT	UT ~ HD
SC ~ LL			*	*	*	*	*
LL ~ UL			*	*	*	*	*
UL ~ LT	*	*		*	*	*	*
LT ~ MLT	*	*	*		*	*	*
MLT ~ MUT	*	*	*	*		*	*
MUT ~ UT	*	*	*	*	*		*
UT ~ HD	*	*	*	*	*	*	

(c) Effect on of trunk-bending direction the net moment calculated via bottom-up approach

Directions	Left	Anterior-Left	Anterior	Anterior-Right	Right
Left			*		
Anterior-Left					
Anterior	*				*
Anterior-Right					
Right			*		

(d) Effect of trunk-bending direction on the net moment calculated via top-down approach

Directions	Left	Anterior-Left	Anterior	Anterior-Right	Right
Left			*		
Anterior-Left					
Anterior	*				*
Anterior-Right					
Right			*		

moment of 60 N·m at the $L5/S1$ joint for an individual during a lifting task. Our results indicate a peak sagittal moment of 52.5 ± 25.7 N·m (0.7 ± 0.2 N·m/kg normalized by body mass) during trunk-bending in the anterior direction, which is in good agreement with previously reported values.

4.1. 3D inter-segmental moments and effect of joint level and trunk-bending direction

The sagittal and coronal moments increased from the superior joints caudally toward the LL ~ UL joint (Tables 1, 2a and b). These results were expected since the inferior joints bear more weight during trunk bending. A significantly larger coronal moment was generated at LL ~ UL compared to SC ~ LL. A similar trend was observed for the sagittal moments but was found to be non-significant. This trend could be due to the fact that, during trunk bending (especially in the lateral directions), the lumbar spine's curvature is at its maximum at the LL ~ UL joint.

In addition, the sagittal and coronal moments were significantly larger than the transverse moment. This likely reflects the nature of the trunk-bending task in which the participants were asked to maintain the spine's torsional direction during the task of reaching for the target. Although participants initially rotated their head/trunk to look at the target, they did not perform a compound flexion/rotation motion during the arc movement. The larger transverse moment in UT ~ HD compared to all other joints occurred because the participants axially rotated their neck to look at a target while moving towards it (Tables 1 and 2c).

4.2. STA effect on inter-segmental net joint moment

The RMS difference (between joint moments obtained before and after compensation for STA effects) for both the SC ~ LL and the LL ~ UL joints was significantly larger compared to the superior joints. Moreover, the RMS difference significantly decreased from the inferior joints to the superior joints, from which we can infer that the most superior joints had the smallest RMS difference. This finding suggests that STA compensation is more important to the assessment of the inferior joints kinetics than it is for the assessment of the superior joints (Tables 4, 5a and b).

The interaction effect of joint level and trunk-bending direction showed that the RMS difference between the calculated lumbar joint (SC ~ LL, LL ~ UL) moments tended to decrease with more lateral trunk-bending directions before and after STA error compensation (Tables 4, 5c and d). This could be explained by the fact that, in the lumbar region, the connection between the thoracolumbar fascia and posterior ligaments assists the motion of the vertebral column during trunk flexion. Therefore, a change in length of these tissues could increase the STA-induced error in this region. Moreover, this RMS difference for mid-upper thoracic levels (MLT ~ MUT and MUT ~ UT) tended to be larger for more lateral trunk-bending directions. This could be because the muscles in the thoracic region (such as the trapezius muscle) are more involved in lateral movements [2], which could increase the STA induced error in this region.

In addition, the RMS difference between the joint moments calculated before and after STA error compensation was significantly smaller in the top-down approach compared to the bottom-up approach. Indeed, in the top-down approach, the kinematics of the inferior segment were calculated with respect to the superior segment. Since the motion and moments of superior joints were significantly less affected by STA-induced errors compared to the inferior joints, error propagation was smaller for the top-down approach than it was for the bottom-up approach. Note that the STA compensation model adopted from [2] assumed that the STA is proportional to the trunk-bending angle, being maximum at the maximum trunk-bending posture. The suitability of more complex models (higher-order polynomials) for compensating STA could be investigated in the future.

4.3. Inter-participant variability

Our results showed that inter-segmental joint moments obtained using a multi-segment model of the HAT have complex, task-specific patterns across different joint levels and trunk-bending directions. These patterns cannot be observed using one- or two-segment HAT models. Despite the homogenous population (individuals with no history of spine-related impairment), we observed high inter-participant variability (CV% > 25% [31]) in peak moments, when the moment magnitude was small (CV% of up to 82.1%, 72.2%, and 59.3% for the sagittal, coronal, and transverse moments, respectively). While previous studies reported high inter-participant variability for spine motion [4], the present study reported, for the first time, the inter-participant variability of the joint moments in a seven-segment HAT model. Notably, the high inter-participant variability of inter-vertebral motion and moment is an impediment to finding consistent normal or pathological patterns for clinical evaluations. A higher inter-participant variability is expected for voluntary tasks (e.g., trunk bending) compared to semi-automatic motor tasks (e.g., walking), and for the small-size, mixed-gender sample used here. Moreover, the inter-participant variability of the joint moments may be affected by the number of trials performed for each participant and task. Preuss et al. [14] suggested that asymmetrical inter-segmental motion patterns during lateral trunk bending can indicate the risk of developing low-back pain. Similarly, the bilateral symmetry of the inter-segmental moment patterns observed in the present study could be used as normative data in clinical evaluations to identify pathological asymmetrical patterns at different levels of the spinal column in patients. In the present study, the calculated joint moments are presented in the global reference frame. However, these joint moments can be later transferred to any other local frames of reference depending on the clinical application. Finally, the data used in this study were collected from a relatively small, mixed-gender population, which limits any generalization for representing either healthy male or female populations. A larger population would be needed to identify any clinically meaningful patterns as normative data for clinical evaluations in the future.

5. Conclusion

This study provided a less erroneous assessment of the 3D inter-segmental moments in a multi-segment HAT model using an optimized estimation of individual-specific BSPs along with compensation of STA-induced errors. The results of this study revealed complex, task-specific patterns for the 3D inter-segmental moments with high inter-participant variability, which could not be studied using single-segment models or without error compensations. Interpretation of the obtained inter-segmental moments can be of great importance for clinical evaluations and developing injury prevention and rehabilitation strategies.

Conflict of interest

None.

Acknowledgements

This work was financially supported by the Natural Sciences and Engineering Research Council of Canada (grant number: RGPIN-2016-04106) and Alberta Innovates Technology Futures. The authors would like to acknowledge assistance of Ms. Gabriella Ueno in pre-processing the data.

Appendix A. Supplementary data

Supplementary material related to this article can be found, in the

online version, at doi:https://doi.org/10.1016/j.gaitpost.2018.06.027.

References

[1] N. Arjmand, D. Gagnon, A. Plamondon, A. Shirazi-Adl, C. Larivière, Comparison of trunk muscle forces and spinal loads estimated by two biomechanical models, Clin. Biomech. 24 (2009) 533–541, http://dx.doi.org/10.1016/j.clinbiomech.2009.05.008.

[2] S. Mahallati, H. Rouhani, R. Preuss, K. Masani, M.R. Popovic, Multisegment kinematics of the spinal column: soft tissue artifacts assessment, J. Biomech. Eng. 138 (2016) 071003, , http://dx.doi.org/10.1115/1.4033545.

[3] S. Schmid, B. Bruhin, D. Ignasiak, J. Romkes, W.R. Taylor, S.J. Ferguson, R. Brunner, S. Lorenzetti, Spinal kinematics during gait in healthy individuals across different age groups, Hum. Mov. Sci. 54 (2017) 73–81, http://dx.doi.org/10.1016/j.humov.2017.04.001.

[4] J.P. Callaghan, A.E. Patla, S.M. McGill, Low back three dimensional joint forces, kinematics, and kinetics during walking, Clin. Biomech. 14 (1999) 203–216.

[5] B.D. Hendershot, E.J. Wolf, Three-dimensional joint reaction forces and moments at the low back during over-ground walking in persons with unilateral lower-extremity amputation, Clin. Biomech. 29 (2014) 235–242, http://dx.doi.org/10.1016/j.clinbiomech.2013.12.005.

[6] C. Larivière, D. Gagnon, P. Loisel, A biomechanical comparison of lifting techniques between subjects with and without chronic low back pain during freestyle lifting and lowering tasks, Clin. Biomech. 17 (2002) 89–98, http://dx.doi.org/10.1016/S0268-0033(01)00106-1.

[7] T. Robert, L. Chèze, R. Dumas, J.P. Verriest, Validation of net joint loads calculated by inverse dynamics in case of complex movements: application to balance recovery movements, J. Biomech. 40 (2007) 2450–2456, http://dx.doi.org/10.1016/j.jbiomech.2006.11.014.

[8] B.D. Hendershot, E.J. Wolf, Persons with unilateral transfemoral amputation have altered lumbosacral kinetics during sitting and standing movements, Gait Posture 42 (2015) 204–209, http://dx.doi.org/10.1016/j.gaitpost.2015.05.011.

[9] A. Plamondon, M. Gagnon, P. Desjardins, Validation of two 3-D segment models to calculate the net reaction forces and moments at the L5/S1 joint in lifting, Clin. Biomech. 11 (1996) 101–110, http://dx.doi.org/10.1016/0268-0033(95)00043-7.

[10] I. Kingma, M.P. De Looze, H.M. Toussaint, H.G. Klijnsma, T.B.M. Bruijnen, Validation of a full body 3-D dynamic linked segment model, Hum. Mov. Sci. 15 (1996) 833–860, http://dx.doi.org/10.1016/S0167-9457(96)00034-6.

[11] J. Seay, W.S. Selbie, J. Hamill, In vivo lumbo-sacral forces and moments during constant speed running at different stride lengths, J. Sports Sci. 26 (2008) 1519–1529, http://dx.doi.org/10.1080/02640410802298235.

[12] D.J. Pearsall, J.G. Reid, L. a Livingston, Segmental inertial parameters of the human trunk as determined from computed tomography, Ann. Biomed. Eng. 24 (1996) 198–210, http://dx.doi.org/10.1007/BF02667349.

[13] R. Fernandes, P. Armada-da-Silva, A. Pool-Goudaazward, V. Moniz-Pereira, A.P. Veloso, Three dimensional multi-segmental trunk kinematics and kinetics during gait: test-retest reliability and minimal detectable change, Gait Posture 46 (2016) 18–25, http://dx.doi.org/10.1016/j.gaitpost.2016.02.007.

[14] R.A. Preuss, M.R. Popovic, Three-dimensional spine kinematics during multi-directional, target-directed trunk movement in sitting, J. Electromyogr. Kinesiol. 20 (2010) 823–832, http://dx.doi.org/10.1016/j.jelekin.2009.07.005.

[15] R. Riemer, E.T. Hsiao-Wecksler, Improving joint torque calculations: optimization-based inverse dynamics to reduce the effect of motion errors, J. Biomech. 41 (2008) 1503–1509, http://dx.doi.org/10.1016/j.jbiomech.2008.02.011.

[16] P.D. Steven, T. McCaw, Errors in alignment of center of pressure and foot coordinates affect predicted lower extremity torques, J. Biomech. 28 (1995) 985–988.

[17] R. Riemer, E.T. Hsiao-Wecksler, Improving net joint torque calculations through a two-step optimization method for estimating body segment parameters, J. Biomech. Eng. 131 (2009), http://dx.doi.org/10.1115/1.3005155 0110071–011007.

[18] R. Riemer, E.T. Hsiao-Wecksler, X. Zhang, Uncertainties in inverse dynamics solutions: a comprehensive analysis and an application to gait, Gait Posture 27 (2008) 578–588, http://dx.doi.org/10.1016/j.gaitpost.2007.07.012.

[19] P. Desjardins, A. Plamondon, M. Gagnon, Sensitivity analysis of segment models to estimate the net reaction moments at the L5/S1 joint in lifting, Med. Eng. Phys. 20 (1998) 153–158, http://dx.doi.org/10.1016/S1350-4533(97)00036-2.

[20] A. Leardini, L. Chiari, U. Della, A. Cappozzo, Human movement analysis using stereophotogrammetry part 3. Soft tissue artifact assessment and compensation, Gait Posture 21 (2005) 212–225, http://dx.doi.org/10.1016/j.gaitpost.2004.05.002.

[21] K.B. Smale, B.M. Potvin, M.S. Shourijeh, D.L. Benoit, Knee joint kinematics and kinetics during the hop and cut after soft tissue artifact suppression: time to reconsider ACL injury mechanisms? J. Biomech. (2017) 1–8, http://dx.doi.org/10.1016/j.jbiomech.2017.06.049.

[22] M.Y. Kuo, T.Y. Tsai, C.C. Lin, T.W. Lu, H.C. Hsu, W.C. Shen, Influence of soft tissue artifacts on the calculated kinematics and kinetics of total knee replacements during sit-to-stand, Gait Posture 33 (2011) 379–384, http://dx.doi.org/10.1016/j.gaitpost.2010.12.007.

[23] K. Matsui, K. Shimada, P.D. Andrew, Deviation of skin marker from bone target during movement of the scapula, J. Orthop. Sci. 11 (2006) 180–184, http://dx.doi.org/10.1007/s00776-005-1000-y.

[24] J.L. Durkin, J.J. Dowling, Analysis of body segment parameter differences between four human populations and the estimation errors of four popular mathematical models, J. Biomech. Eng. ASME 125 (2003) 515–522, http://dx.doi.org/10.1115/1.1590359.

[25] S. Chen, H. Hsieh, T. Lu, C. Tseng, A method for estimating subject-specific body segment inertial parameters in human movement analysis, Gait Posture 33 (2011) 695–700, http://dx.doi.org/10.1016/j.gaitpost.2011.03.004.

[26] A.H. Vette, T. Yoshida, T.A. Thrasher, K. Masani, M.R. Popovic, A comprehensive three-dimensional dynamic model of the human head and trunk for estimating lumbar and cervical joint torques and forces from upper body kinematics, Med. Eng. Phys. 34 (2012) 640–649, http://dx.doi.org/10.1016/j.medengphy.2011.11.023.

[27] A. Noamani, A.H. Vette, R. Preuss, M.R. Popovic, H. Rouhani, Optimal estimation of anthropometric parameters for quantifying multi-segment trunk kinetics, J. Biomech. Eng. (2018), http://dx.doi.org/10.1115/1.4040247 (Accepted).

[28] A.H. Vette, T. Yoshida, T.A. Thrasher, K. Masani, M.R. Popovic, A complete, non-lumped, and verifiable set of upper body segment parameters for three-dimensional dynamic modeling, Med. Eng. Phys. 33 (2011) 70–79, http://dx.doi.org/10.1016/j.medengphy.2010.09.008.

[29] R.N. Hinrichs, Regression equations to predict segmental moments inertia from anthropometric measurements: extension of the data of chandler Et Al, J. Biomech. 18 (1985) (1975) 621–624.

[30] T.C. Pataky, V.M. Zatsiorsky, J.H. Challis, A simple method to determine body segment masses in vivo : reliability, accuracy and sensitivity analysis, Clin. Biomech. 18 (2003) 364–368, http://dx.doi.org/10.1016/S0268-0033(03)00015-9.

[31] H. Rouhani, J. Favre, X. Crevoisier, B.M. Jolles, K. Aminian, Segmentation of foot and ankle complex based on kinematic criteria, Comput. Methods Biomech. Biomed. Engin. 14 (2011) 773–781, http://dx.doi.org/10.1080/10255842.2010.494161.